Real-Time Speckle and Impulsive Noise Suppression in 3-D Ultrasound Imaging

Francisco J. Gallegos-Funes, Jose M. de-la-Rosa-Vazquez,
Alberto J. Rosales-Silva and Suren Stolik Isakina
National Polytechnic Institute of Mexico
Mexico

1. Introduction

Ultrasound imaging is considered one of the most powerful techniques for medical diagnosis and is often preferred over other medical imaging modalities because of noninvasive, portable, versatile and low-cost properties (Webb, 2002; Abd-Elmoniem, 2002; Porter, 2001; Shekhar, 2002). A fundamental problem in the field of ultrasound imaging is the speckle noise influence, which is a major limitation on image quality in ultrasound imaging. Imaging speckle is a phenomenon that occurs when a coherent source and a noncoherent detector are used to interrogate a medium, which is rough on the scale of the wavelength. Speckle noise occurs especially in images of the liver and kidney whose underlying structures are too small to be resolved using long ultrasound wavelength. The presence of speckle noise affects the human interpretation of the images as well the accuracy of computer-assisted diagnostic techniques (Nikolaidis, 2000; Kim & Park, 2001)

The goal of this chapter is the capability and real-time processing features of the robust MM-L (Median M-type L) filters to remove speckle and impulsive noise in 3-D ultrasound images (Gallegos-Funes et al., 2008, Varela-Benitez et al., 2007). The Texas Instruments DSP TMS320C6711 is used to implement the algorithms (Texas Instruments, 1998; Kehtarnavaz, 2001). Based on the processing time values of each a 3-D filter, different configurations of sweeping cubes (voxels) are used to obtain a balance between the processing time and quality of the restoration of 3-D images (Nikolaidis, 2000). The criteria used to measure the performance of filters are: the peak signal-to-noise ratio (PSNR) to characterize the noise suppression, and the mean absolute error (MAE) to evaluate the preservation of edges and fine details (Bovik, 2000; Astola & Kuosmanen, 1997; Kotropoulos & Pitas, 2001; Pitas & Venetsanopoulos, 1990). Extensive simulation results have demonstrated that the proposed filters can consistently outperform other filters used as comparative by balancing the tradeoff between noise suppression, detail preservation, and processing time.

2. Problem formulation

All coherent imaging that include laser, SAR, and ultrasound imagery are affected by speckle noise (Abd-Elmoniem, 2002; Bovik, 2000; Kotropoulos & Pitas, 2001). Speckle may appear distinct in different imaging systems but it is always manifested in granular pattern due to image formation under coherent waves. A general model for ultrasound speckle noise can be written as (Abd-Elmoniem, 2002),

$$x(i,j) = S(i,j)\eta_m(i,j) + \eta_a(i,j) \tag{1}$$

where $x(i,j)$ is a noisy observation (i.e., the recorded ultrasound image) of the two-dimensional (2-D) function $S(i,j)$ (i.e., the noise-free image that has to be recovered), $\eta_m(i,j)$ and $\eta_a(i,j)$ are the corrupting multiplicative and additive speckle noise components, respectively, and i and j are variables of spatial locations that belong to 2-D space of all real numbers $(i,j) \in \Re^2$. Generally, the effect of the additive component (such as sensor noise) of the speckle in ultrasound images is less significant than the effect of the multiplicative component (coherent interference). Thus, ignoring the term $\eta_a(i,j)$, can be rewritten (1) as (Abd-Elmoniem, 2002),

$$x(i,j) = S(i,j)\eta_m(i,j). \tag{2}$$

To transform the multiplicative noise model into the additive noise model, we apply the logarithmic function on both sides of (2)

$$\log x(i,j) = \log S(i,j) + \log \eta_m(i,j), \tag{3}$$

or

$$x^l(i,j) = S^l(i,j)\eta_m^l(i,j), \tag{4}$$

where $\eta_m^l(x,y)$ is approximated as additive white noise. We assume here that the speckle pattern has a white Gaussian noise model. Therefore, the acquisition or transmission of digitized images through sensor or digital communication link is often interfered by impulsive noise (Astola & Kuosmanen, 1997; Pitas & Venetsanopoulos, 1990). Thus, the impulsive noise is added to the model (2) as follows (Astola & Kuosmanen, 1997)

$$x(i,j) = \eta_i\big(S(i,j)\eta_m(i,j)\big) \tag{5}$$

where $\eta_i(f(i,j))$ is the functional $\eta_i(f(i,j)) = \begin{cases} random\ valued\ spike\ with\ probability\ P \\ f(i,j)\ \ otherwise \end{cases}$.

3. 3-D Median M-type L-filters

Consider the monochromatic 3-D image $x(i,j,k)$ where i and j are the 2-D spatial axes and k is the time axis or may be the third dimension for 3-D images (Nikolaidis & Pitas, 2000; Kim & Park, 2001). When the current pixel location is (i,j,k), a 11-point window $W(i,j,k)$, is defined as follows (Kim & Park, 2001):

$$W(i,j,k) = \big\{ x(i-1,j-1,k), x(i,j-1,k), x(i+1,j-1,k), x(i-1,j,k), x(i,j,k), x(i+1,j,k), \\ x(i-1,j+1,k), x(i,j+1,k), x(i+1,j+1,k), x(i,j,k+1), x(i,j,k-1) \big\} \tag{6}$$

From eq. (6), the window $W(i,j,k)$ includes a 3x3 window centered at the current pixel of the current frame and the current pixel's corresponding pixels in the previous and the next frames, as shown in Figure 1.
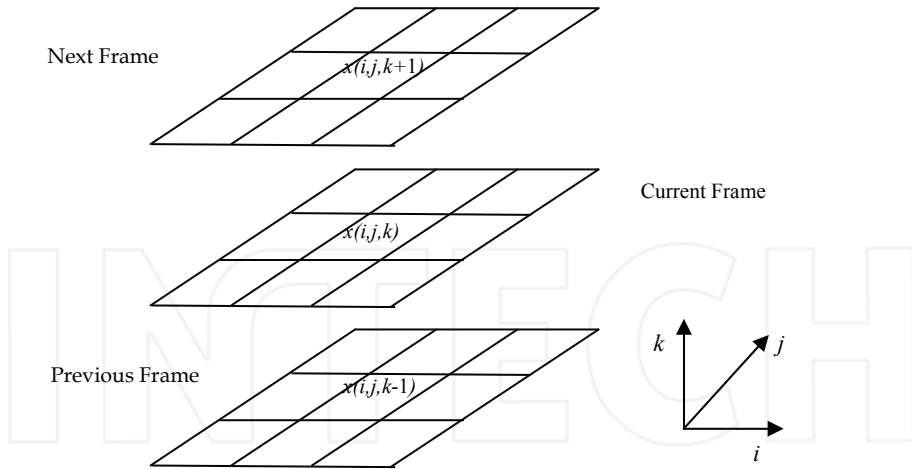
Fig. 1. The elements of the 11-point window $W(i,j,k)$.

A 3-D image can be considered as a 3-D matrix $x[i][j][k]$ or $x(i,j,k)$ of dimensions $N_1 \times N_2 \times N_3$ where i, j, k denote row, column, and slice (image) coordinates, respectively (Nikolaidis & Pitas, 2000). The 3-D representation is depicted in Figure 2. Each a voxel (volume elements) has physical size $di \times dj \times dk$ physical units (e.g. mm^3 or μm^3).

Recently (Gallegos & Ponomaryov, 2004; Gallegos et al., 2005), we proposed the combined RM (Rank M-type) –estimators for applications in image noise suppression. These estimators use the *M*-estimator combined with the *R*-estimator, such as the median or ABST (Ansari-Bradley-Siegel-Tukey) estimator. It was demonstrated that the robust properties of the RM-estimators exceed the robust properties of the base *R*- and *M*- estimators for the impulsive and speckle noise suppression (Gallegos & Ponomaryov, 2004). The RM-estimator used in the proposed 3-D filtering scheme is presented in such a form (Gallegos & Ponomaryov, 2004; Gallegos et al., 2005):

$$\theta_{\text{medM}} = \text{MED}\left\{ X_p \tilde{\psi}\left(X_p - \text{MED}\{\mathbf{X}\} \right), \ p=1,\ldots,N \right\} \tag{7}$$

where θ_{medM} is the Median M-type (MM) estimator, X_p are data samples, $p = 1,\ldots,N$, $\tilde{\psi}$ is the normalized function $\psi: \psi(X) = X\tilde{\psi}(X)$, and $\vec{X}$ is the primary data sample.

The MM-L type filter has been designed using the MM-estimator to increase the robustness of the *L*-filter. The detail description of such a filtering scheme is presented in recent works (Gallegos-Funes et al., 2008; Varela-Benitez et al., 2007), and in here we propose its modifications for 3-D imaging applications. So, the 3-D MM-L (Median M-type L) filter is defined as follows:

$$\hat{f}_{RM\text{-}L}(i,j,k) = \frac{\text{med}\left\{ a_p \left[X_p \cdot \psi\left(X_p - \text{med}\{\vec{X}\} \right) \right] \right\}}{a_{\text{med}}}, \tag{8}$$
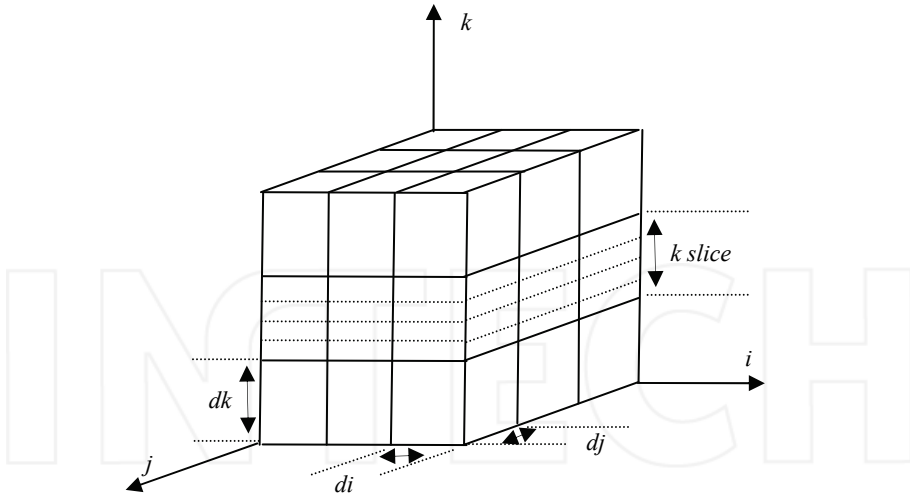
Fig. 2. 3-D representation as a 3-D array.

where $X_p \cdot \psi\left(X_p - \mathrm{med}\{\vec{X}\}\right)$ represent the selected pixels in accordance with the influence function into a rectangular 3-D grid of voxels, $a_p = \int_{p-1/n}^{p/n} h(\lambda) d\lambda \big/ \int_0^1 h(\lambda) d\lambda$ are the weighted coefficients where $h(\lambda)$ is a probability density function, a_{med} is the median of coefficients a_p, the filtering 3-D grid size is $N_1 \times N_2 \times N_3$, $N_p = (2L+1)^2$ and $l_p, m_p, n_p = -L, \ldots, L$, and X_p is the input data sample from the $x(i,j,k)$ of the 3-D image contaminated by noise in the rectangular 3-D grid where i and j are the 2-D spatial axes and k is the time axis (or third dimension). We use in the proposed 3-D filter the Tukey biweight influence function defined as (Hampel et al., 1986; Huber, 1981),

$$\psi_{\mathrm{bi}(r)}(X) = \begin{cases} X^2\left(r^2 - X^2\right), |X| \le r \\ 0, |X| > r \end{cases} \tag{9}$$

where r is connected with the range of $\psi(X)$.

To improve the properties of impulsive noise suppression of the proposed MM L-filter we introduced an impulsive detector, this detector chooses if that voxel is filtered. The impulsive detector used here is defined as (Aizenberg et al., 2003):

$$\left[\left(rank\left(X_{ijk}\right) \le T_1\right) \vee \left(rank\left(X_{ijk}\right) \ge N_p - T_1\right)\right] \wedge \left|X_{ijk} - \mathrm{MED}\left(\vec{X}\right)\right| \ge T_2 , \tag{10}$$

where X_{ijk} is the central voxel in the 3-D grid, $T_1 > 0$ and $T_2 \ge 0$ are thresholds.

We noted that the weighted coefficients of proposed 3-D filter are calculated using the exponential, Laplacian, and Uniform distribution functions (Pitas & Venetsanopoulos, 1990; Hampel et al., 1986) by each sliding filter window because the influence function selects

which pixels are used and then compute the weighted coefficients of *L*-filter according with the number of pixels used into the filtering window.

The parameters of the 3-D MM L-filters were found after numerous simulations by means of use a 3x3x3 grid (i.e., $N_1 \times N_2 \times N_3 = 27$, $l, m, n = -1, \ldots, 1$, and $N_p = (2L + 1)^2 = 9$). The idea was to find the parameters values when the criteria PSNR and MAE should be optimum. The optimal parameters of proposed filters are: $T_1=3$ and $T_2=15$ for the impulsive detector, and *r=15* for Tukey influence function.

Processing times may change when we use other values for the parameters, increasing or decreasing processing times. The PSNR and MAE values change within the range of $\pm(5-10)\%$, it is due to the proposed fixed parameters that can realize the real-time implementation of the 3-D MM L-filters.

4. Experimental results

The objective criteria employed to compare the performance of noise suppression of different filters was the *peak signal to noise ratio* (PSNR) and for the evaluation of fine detail preservation the *mean absolute error* (MAE) (Bovik, 2000; Pitas & Venetsanopoulos, 1990):

$$PSNR = 10 \cdot \log\left[\frac{(255)^2}{MSE}\right], \ \ dB \tag{11}$$

$$MAE = \frac{1}{N_1 N_2 N_3} \sum_{i=0}^{N_1-1} \sum_{j=0}^{N_2-1} \sum_{k=0}^{N_3-1} \left| S(i,j,k) - \hat{f}(i,j,k) \right| \tag{12}$$

where $MSE = \frac{1}{N_1 N_2 N_3} \sum_{i=0}^{N_1-1} \sum_{j=0}^{N_2-1} \sum_{k=0}^{N_3-1} \left[S(i,j,k) - \hat{f}(i,j,k) \right]^2$ is the *mean square error*, $S(i,j,k)$ is

the original free noise 3-D image, $\hat{f}(i,j,k)$ is the restored 3-D image, and N_1, N_2, N_3 are the

sizes of the 3-D image.

The runtime analysis of the 3-D MM L-filters and other concerned filters used as comparative were implemented by using the Texas Instruments DSP TMS320C6711 (Texas Instruments, 1998). This DSP has a performance of up to 900 MFLOPS at a clock rate of 150 MHz. The filtering algorithms were implemented in C language using the BORLANDC 3.1 for all routines, data structure processing and low level I/O operations. Then, we compiled and executed these programs in the DSP TMS320C6711 applying the Code Composer Studio 2.0. The processing time in seconds includes the time for acquisition, processing, and storing data.

The described 3-D MM L-filters with Tukey biweight influence function and different distribution functions have been evaluated, and their performance has been compared with different nonlinear 2-D filters which were adapted to 3-D. The filters used as comparative were the *modified a-Trimmed Mean* (Astola & Kuosmanen, 1997; Bednar & Watt, 1984), *Ranked-Order* (RO) (Astola & Kuosmanen, 1997; Pitas & Venetsanopoulos, 1990), *Multistage Median* (MSM1 to MSM6) (Arce, 1991), *Comparison and Selection* (CS) (Astola & Kuosmanen, 1997; Pitas & Venetsanopoulos, 1990), *MaxMed* (Nieminen & Neuvo, 1988), *Selection Average* (SelAve) (Astola & Kuosmanen, 1997; Pitas & Venetsanopoulos, 1990), *Selection Median* (SelMed) (Astola & Kuosmanen, 1997; Pitas & Venetsanopoulos, 1990), *Lower-Upper-Middle* (LUM, LUM Sharp, and LUM Smooth) (Hardie & Boncelet, 1993), and *Rank M-type K-nearest*

Neigbour (RM-KNN) (Ponomaryov et al., 2006) filters. These filters were computed according to their references and were adapted to 3-D imaging. Several experiments were realized to investigate the performances of the different techniques in 3-D imaging (Varela-Benitez et al., 2007).

4.1 Experiment 1

Figure 3 shows the 3-D space used to reconstruct the human organ as an object into 3-D space with its real measures. The coordinate z represents each a 2-D image of the sweeping in the 3-D space, and the coordinates x and y represent the height and width of the 2-D image, respectively. Having the 3-D image, one can carry out courts in the different plane yz, xy, and xz.
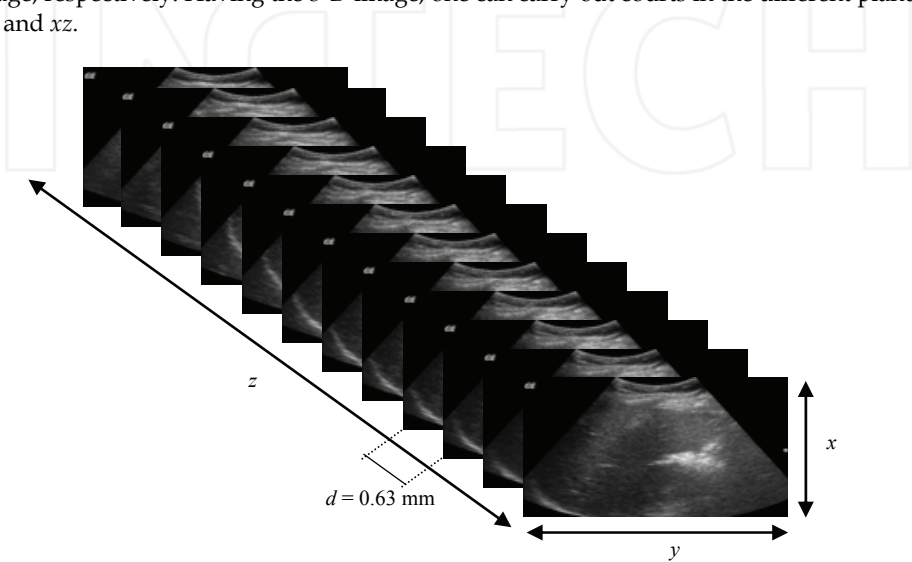

Fig. 3. 3-D ultrasound image representation.

The experiment 1 was realized by degraded an ultrasound sequence of 640x480 pixels with 90 frames (3-D image of 640x480x90 voxels) with 5 and 20% of impulsive noise and with the natural speckle noise of the 3-D image.

Table 1 presents the performance results of proposed filters and the comparative results of different non linear filters applied to a frame of the original sequence. From Table 1 we observe that when the noise corruption is 5%, the proposed filters almost have the same performances that other filters in terms of noise suppression and detail preservation, but when the noise corruption is high the best results are given by the MM-KNN filters. It can be seen from Table 1 that the processing time for proposed filters is less in comparison with the MM-KNN filters but the times of proposed ones are large in comparison with other filters. It is easy to see that the processing time values for MM L-filters are decreased but the performance criteria PSNR and MAE are sufficiently acceptable (see Table 1) in comparison with other RM filters such as the RM-KNN (Median, Wilcoxon, and ABST –KNN) filters and other filters proposed as comparative.

3-D Filters	Impulsive noise percentage					
	5%			20%		
	PSNR	MAE	Time	PSNR	MAE	Time
LUM Smooth	29.94	2.75	4.122	25.26	4.87	5.754
LUM Sharp	17.36	17.28	4.224	15.90	20.17	5.867
LUM	18.53	15.51	4.317	17.59	17.68	5.984
MaxMed	27.10	6.24	1.1981	23.24	9.20	1.1981
Modified Trimmed Mean	24.90	7.04	2.1716	24.71	7.35	2.1716
MSM1	28.92	4.25	0.5846	26.68	5.30	0.5846
MSM2	28.13	5.06	0.5773	26.18	6.00	0.5773
MSM3	27.46	5.94	1.2681	26.88	6.46	1.2681
MSM4	27.94	5.33	1.2367	27.13	5.81	1.2367
MSM5	29.44	3.77	1.2198	25.98	5.17	1.2198
MSM6	28.29	5.06	1.1667	27.67	5.45	1.1667
SelAve	26.83	6.97	1.9620	22.34	14.33	1.9620
SelMed	27.43	5.63	2.3240	26.31	6.37	2.3240
RO	26.50	6.67	1.6836	26.27	6.94	1.6836
MM-KNN Cut	28.83	4.27	20.49	27.91	5.14	20.63
MM-KNN Hampel	28.79	4.31	20.51	27.89	5.16	21.26
WM-KNN Hampel	22.75	10.91	38.54	21.98	11.59	45.06
ABSTM-KNN Hampel	27.45	5.21	34.14	26.77	6.00	38.00
MM-L TUKEY Uniform	28.30	4.77	3.7731	25.93	5.69	3.7732
MM-L TUKEY Laplacian	28.03	5.00	3.7733	25.80	5.83	3.7733
MM-L TUKEY	27.52	5.63	3.7732	24.84	7.01	3.7737

Table 1. Performance results of different filters in a frame of ultrasound sequence degraded with impulsive noise.

Figure 4 displays the visual results in terms of restored images obtained by the use of different filters according to Table 1 by means of use the xz plane. In Figure 4, we can see that the proposed MM L-filters provide good results in noise suppression and detail preservation.

4.2 Experiment 2

The experiment 2 was performed in the same sequence but it was degraded with 0.05 and 0.1 of variance of speckle noise added to the natural speckle noise of the sequence. The performance results are depicted in Table 2 by use of a frame in the xy plane of the sequence. From Table 2 we observe that the 3-D MM L-filters provide the best results in comparison to other comparative filters proposed. Figure 5 exhibits the visual results of restored images obtained by use of different filters according to Table 2, we observe that the proposed filters provide the best results in speckle noise suppression and detail preservation in comparison with other filters used.
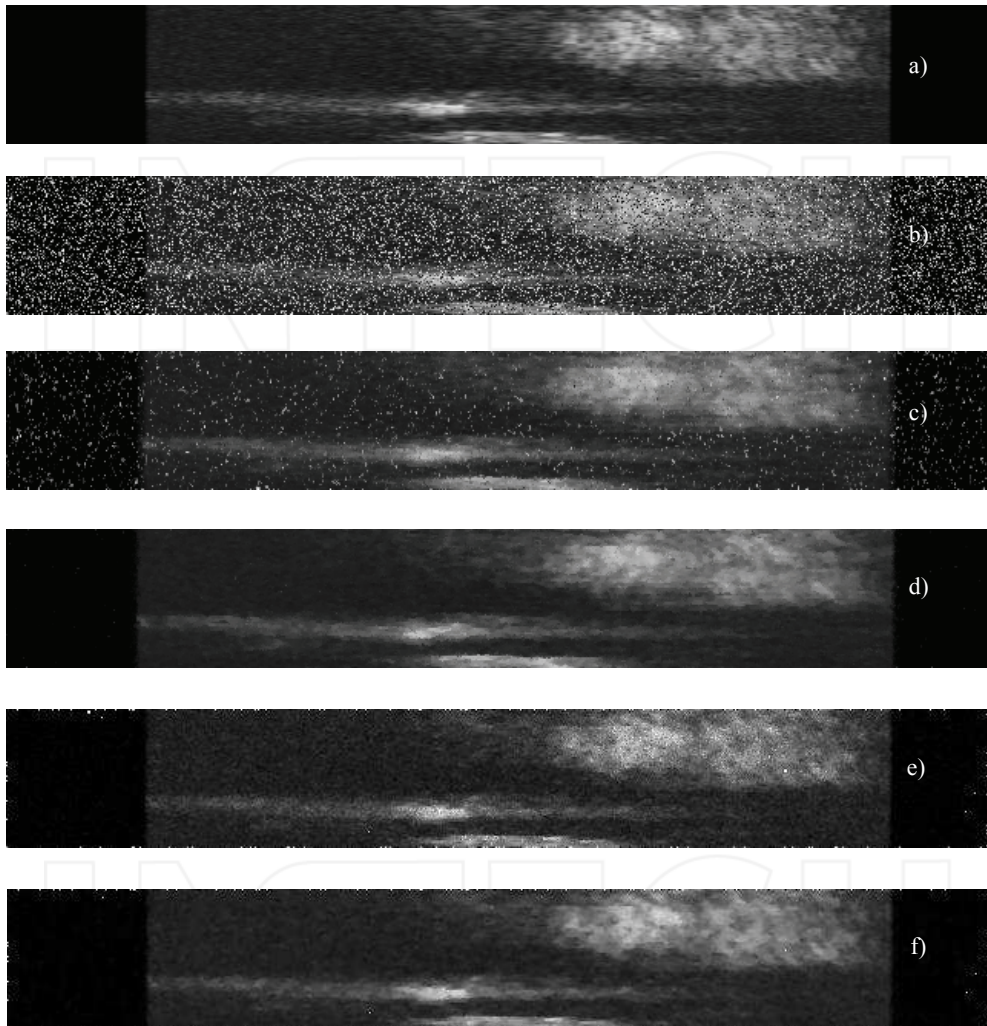
Fig. 4. Visual results in a frame of ultrasound sequence. a) original frame, b) frame degraded by 20% of impulsive noise, c) restored frame by MSM5 filter, d) restored frame by MM-KNN (Hampel) filter, e) restored frame by MM L-filter (Exponential), f) restored frame by MM L-filter (Laplacian).

3-D Filters	Speckle noise variance			
	0.05		0.1	
	PSNR	MAE	PSNR	MAE
CS	15.44	32.88	13.84	39.78
LUM Smooth	17.92	25.14	15.44	33.82
LUM Sharp	15.63	30.93	14.44	36.43
LUM	15.52	31.43	14.38	36.75
MaxMed	18.56	24.21	15.92	32.91
Modified α-Trimmed Mean	20.42	15.12	19.10	18.66
MSM1	20.57	17.62	18.06	23.68
MSM2	20.48	17.79	18.04	23.73
MSM3	22.42	14.21	20.26	18.46
MSM4	21.70	15.40	19.35	20.35
MSM5	19.55	20.21	16.96	27.44
MSM6	22.08	14.69	19.74	19.37
SelAve	21.18	17.65	19.19	22.81
SelMed	20.84	15.75	19.01	20.09
RO	21.59	14.520	19.80	18.18
MM-KNN Hampel	21.57	15.169	19.04	20.80
MM-L TUKEY Uniform	29.88	5.016	28.618	5.743
MM-L TUKEY Laplacian	28.80	5.646	28.19	6.020
MM-L TUKEY Exponential	28.03	6.261	26.30	7.666

Table 2. Performance results of different filters in a frame of ultrasound sequence degraded with speckle noise.
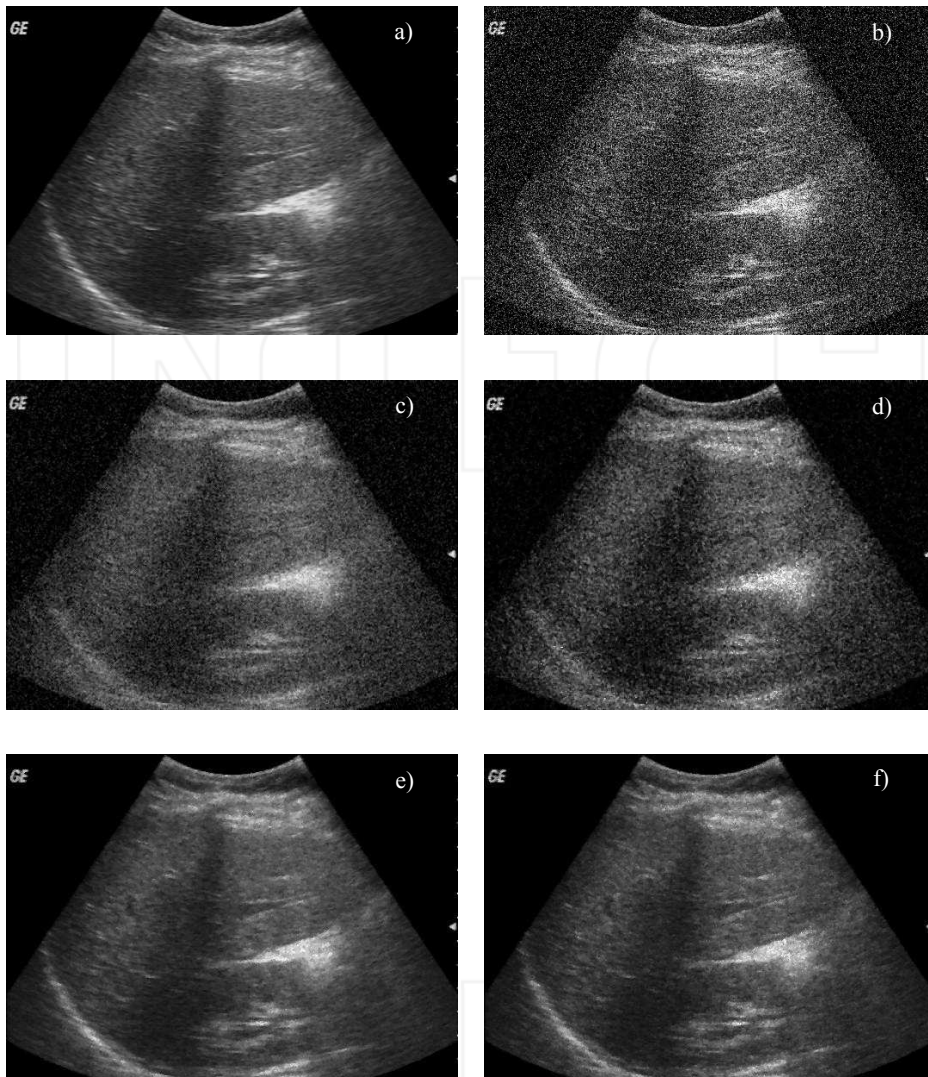
Fig. 5. Visual results in a frame of ultrasound sequence. a) Original frame, b) frame degraded by 0.05 of variance of speckle noise, c) restored frame by MSM6 filter, d) restored frame by MM-KNN filter, e) restored frame by MM L-filter (Uniform), f) restored frame by MM-L filter (Laplacian).

4.3 Experiment 3

Experiment 3 is related to different voxels cube configurations to provide better noise reduction. Figure 6 shows nine configurations of voxels used in the proposed 3-D filtering algorithms. It is obvious that by using less voxels in the different cube configurations the processing time can be decreased. In this experiment the ultrasound sequence was degraded
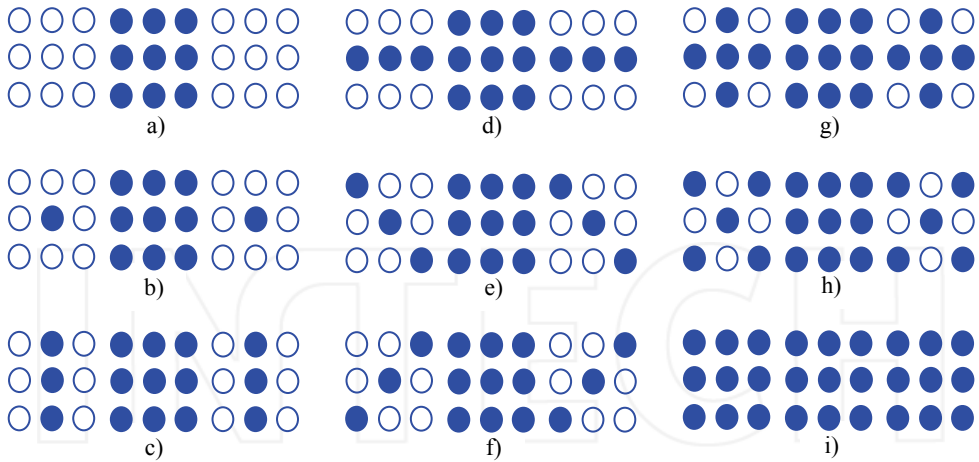
Fig. 6. Different configurations of processing cube.

with 20% of impulsive noise. Then, we implemented different cube configurations in the α-Trimmed Mean, MM-KNN, and MM L filters.

Table 3 presents the performance results of different filters in the case of use different cube configurations in the *xy* plane of the sequence. From this Table, the MM-KNN and α-Trimmed Mean filters provide better results in terms of PSNR in comparison with the MM L-filter but in the MAE performance the proposed filter provides the better results. About the processing time of the algorithms, the proposed MM L-filter has less processing time in comparison with the MM-KNN filter.

4.4 Discussion of results in ultrasound imaging

From the results presented in this chapter (see Tables 1-3) we conclude that the proposed MM L-filters can suppress the speckle noise with detail preservation better than other filters proposed in the literature. In the case of impulsive noise suppression the proposed filters have good performance in comparison with other filters proposed in the literature. Finally, the processing time of MM L-filters is acceptable to process 3-D images in real time applications because the proposed filters can process QCIF video format with standard film velocity for computer vision systems.

4.5 Experiment 4

We also process real video sequences to demonstrate that the proposed method potentially can provide a solution to quality video transmission. In the case of this test we use one frame of the video sequences "Carphone" and "Miss America" that were corrupted by mixed noise of 20% of impulsive noise and 0.1 of variance of speckle noise. The PSNR and MAE performances are depicted in Table 4. The visual results of the processing frames in the case of a frame of video sequence "Carphone" are displayed in Figure 7 according with Table 4.

Voxel Configuration	20% of impulsive noise					
	MM-KNN filter			Modified α-trimmed mean filter		
	PSNR	MAE	Time (secs.)	PSNR	MAE	Time (secs.)
a	28.41	4.54	1.6425	26.32	6.98	0.6398
b	29.41	4.42	1.9082	28.24	5.69	0.7127
c	28.77	5.28	4.8228	28.75	5.49	0.8267
d	28.86	5.16	5.1989	28.88	5.35	0.8269
e	28.71	5.29	4.8159	28.68	5.49	0.8267
f	28.68	5.30	4.8297	28.66	5.50	0.8268
g	28.43	5.23	10.0552	28.30	5.68	1.3775
h	28.19	5.38	10.0775	28.04	5.85	1.3769
i	27.92	5.14	20.6575	25.75	7.76	2.1716

	MM L-filter Uniform		
	PSNR	MAE	Time (secs.)
a	26.83	5.81	1.1485
b	27.67	5.00	1.1627
c	27.57	5.06	2.3251
d	28.30	4.31	2.3247
e	27.53	5.10	2.3289
f	27.54	5.11	2.3254
g	28.07	4.55	3.4934
h	27.44	5.21	3.4993
i	27.77	4.85	4.7732

Table 3. Performance results by use different cube configurations in a frame of ultrasound sequence degraded with impulsive noise.

Filters	20% of impulsive noise and 0.1 of variance of speckle noise			
	Carphone		Miss America	
	PSNR	MAE	PSNR	MAE
MM L Exponential, ND	18.8798	20.4191	21.5452	15.0880
MM L Laplacian, ND	20.4120	16.1230	24.1252	9.1169
MM L Uniform, ND	20.8869	15.1964	24.5764	8.4784
MM L Exponential, D	19.5138	18.6947	22.4313	12.6873
MM L Laplacian, D	20.7843	15.5185	23.9603	9.9071
MM L Uniform, D	21.1308	14.8694	24.5236	8.5236

Table 4. Performance results in a frame of video sequences "Carphone" and "Miss America" degraded with 20% of impulsive noise and 0.1 of variance of speckle noise by the use of different filters, where ND is without noise detector and D is with noise detector.
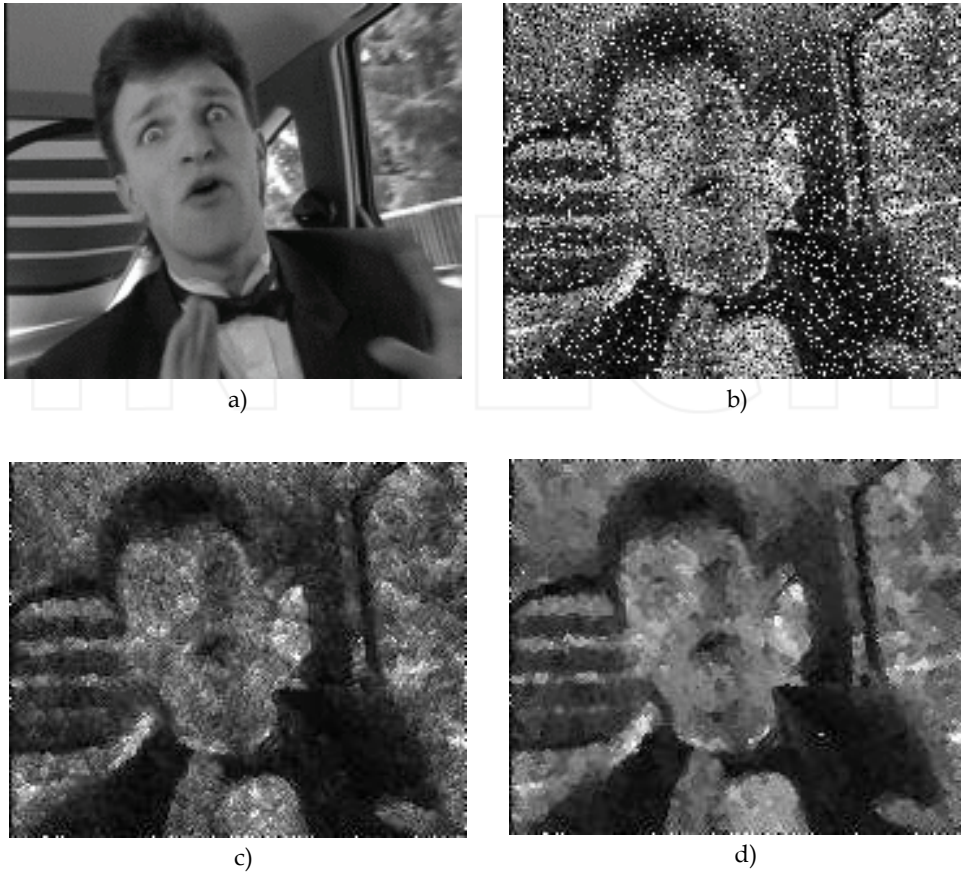
Fig. 7. Visual results in a frame of video sequence "Carphone", a) Original frame of "Carphone", b) Frame degraded with mixed noise of 20% of impulsive noise and 0.1 of variance of speckle noise, c) Restored frame with the proponed filter without noise detector, d) Restored frame with the proposed filter with noise detector.

4.6 Experiment 5

To demonstrate the performance of the proposed filtering scheme we apply it for filtering of the SAR images, which naturally have speckle noise. The results of such a filtering are presented in the Figure 8 in the case of the SAR image "Pentagon". It is possible to see analyzing the filtering images that speckle noise can be efficiently suppressed, while the sharpness and fine feature are preserved using the proposed MM L-filter.
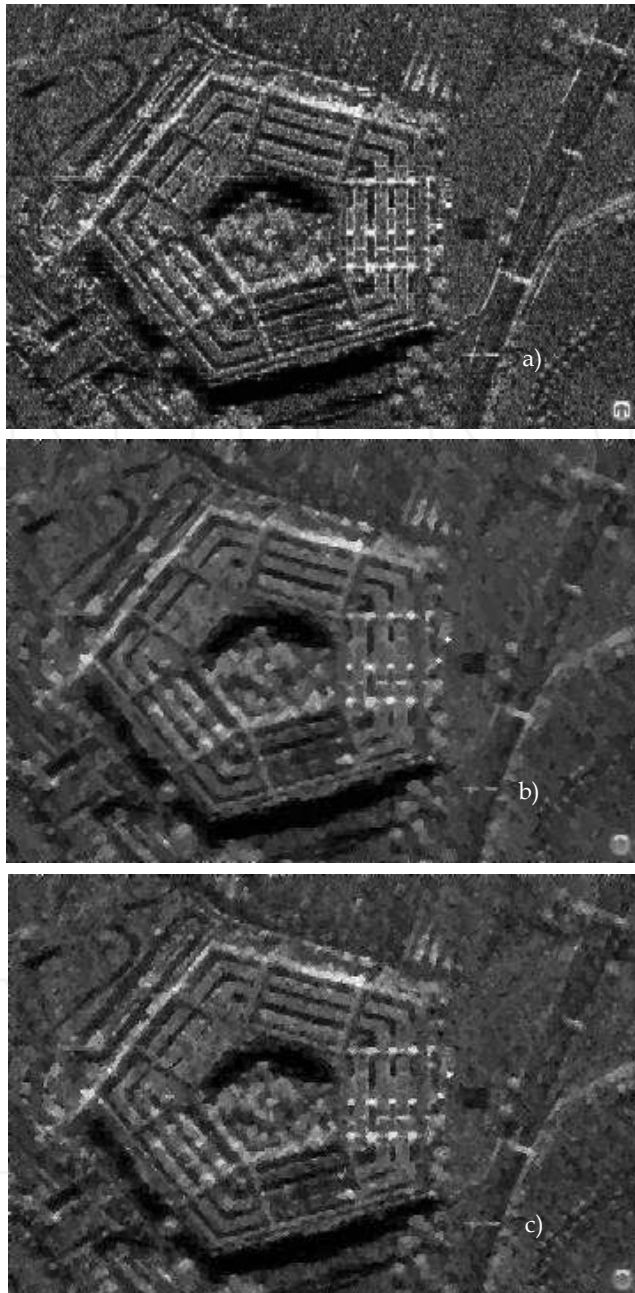
Fig. 8. Comparative results of despeckled SAR image. a) Original image "Pentagon", resolution 1m, source Sandia National Lab., b) Despeckled image with the MM L-filter without noise detector, c) Despeckled image with the MM L-filter with noise detector.

5. Conclusions

In this chapter is presented a real-time implementation of the 3-D MM L-filter for impulsive and multiplicative noise suppression with good detail preservation by means of use of DSP TMS320C6711. Different simulation results have demonstrated that the proposed filters consistently outperform other filters by balancing the tradeoff between speckle and impulsive noise suppression, detail preservation, and processing time. The proposed filter potentially provides a real-time solution to quality video transmission. The use of the linear combinations of order statistics (*L*-filter) with the MM-estimator provide to proposed 3-D MM L-filter better performance in terms of speckle noise in comparison with the 3-D RM-KNN filtering algorithm. In the case of impulsive noise the proposed filter provides good results in comparison with different filters found in scientific literature.

6. References

Abd-Elmoniem, K. Z., Youssef, A. M., & Kadah, Y. M. (2002). Real-Time speckle reduction and coherence enhancement in ultrasound imaging via nonlinear anisotropic diffusion. *IEEE Trans. Biomed. Eng.* Vol.49, No.9, 997-1014, ISSN:0018-9294

Aizenberg, I., Astola, J., Bregin, T., Butakoff, C., Egiazarian, K., & Paily, D. (2003). Detectors of the Impulsive Noise and new Effective Filters for the Impulsive Noise Reduction, *Proc. SPIE Image Process., Algorithms and Syst. II*, Vol. 5014, ISBN: 9780819448149, pp. 419-428, San Jose, Ca, USA

Arce, G. R. (1991). Multistage order statistic filters for image sequence processing. *IEEE Trans. Signal Process.* Vol.39, No.5, 1146-1163, ISSN:1053-587X

Astola, J. & Kuosmanen, P. (1997). *Fundamentals of Nonlinear Digital Filtering,* CRC Press. ISBN:0-8493-2570-6, Boca Raton-New York, USA

Bednar, J. B., & Watt, T. L. (1984). Alpha-trimmed means and their relationship to median filters. *IEEE Trans. Acoust., Speech, and Signal Process,* Vol.ASSP-32, 145-153, ISSN: 0096-3518

Bovik, A. (2000). *Handbook of Image and Video Processing,* Academic Press., ISBN:0121197921, San Diego CA

Gallegos, F., & Ponomaryov, V. (2004). Real-time image filtering scheme based on robust estimators in presence of impulsive noise. *Real Time Imaging*, Vol.8, No.2, 78-90, ISSN:1077-2014

Gallegos-Funes, F., Ponomaryov, V., & De-La-Rosa J. (2005). ABST M-type K-nearest neighbor (ABSTM-KNN) for image denoising. *IEICE Trans. Funds. Electronics Comms. Computer Science*, Vol.E88A, No.3, 798-799, ISSN:0916-8508

Gallegos-Funes, F., Varela-Benitez, J., & Ponomaryov, V. (2008). Rank M-Type L (RM L)-Filter for Image Denoising, *IEICE Trans. Funds. Electronics, Comms. Computer Sciences*, Vol.E91A, No.12, 3817-3819, ISSN:0916-8508

Hampel, F. R., Ronchetti, E. M., Rouseew, P. J. & Stahel, W. A. (1986). *Robust Statistics. The approach based on influence function.* Wiley ISBN:0-471-73577-9, New York, USA

Hardie, R. C., & Boncelet, C. G. (1993). LUM filters: a class of rank order based filters for smoothing and sharpening. *IEEE Trans. Signal Process.* Vol.41, 1061-1076, ISSN:1053-587X

Huber, P.J. (1981). *Robust Statistics,* Wiley, ISBN:0-471-65072-2, New York, USA

Kehtarnavaz, N., & Keramat, M. (2001). *DSP System Design using the TMS320C6000*, Prentice Hall, ISBN:0-13-091031-7, Upper Saddle River, NJ, USA.

Kim, J. S., & Park, H. W. (2001). Adaptive 3-D median filtering for restoration of an image sequence corrupted by impulsive noise. *Signal Processing: Image Communication,* Vol.16, 657-668, ISSN: 0923-5965

Kotropoulos, C. & Pitas, I. (2001). *Nonlinear Model-Based Image/Video Processing and Analysis*, John Wiley & Sons, ISBN:0-471-37735-X, New York

Nieminen, A., & Neuvo, Y. (1988). Comments of theoretical analysis of the max/median filter. *IEEE Trans. Acoust., Speech, and Signal Process.* Vol.ASSP-36, 826-827, ISSN: 0096-3518

Nikolaidis, N., & Pitas, I. (2001). *3-D Image Processing Algorithms*, John Wiley & Sons, ISBN:0-471-37736-8, New York, USA

Pitas, I., & Venetsanopoulos, A. N. (1990). *Nonlinear Digital Filters: Principles and Applications*, Kluwer Academic Publisher, ISBN: 0792390490, Boston, USA

Ponomaryov, V., Gallegos-Funes, F., Sansores-Pech, R., & Sadovnychiy, S. (2006). Real-time Noise suppression in 3D ultrasound Imaging based on Order Statistics. *IEE Electronics Letters*, Vol.42, No.2, 80-82, ISSN:0013-5194

Porter, B. C., Rubens, D. J., Strang, J. G., Smith, J., Totterman, S., & Parker, K. J. (2001). Three-dimensional registration and fusion of ultrasound and MRI using major vessels as fiducial markers. *IEEE Trans. Med. Imag.* Vol.20, No.4, 354-359, ISSN: 0278-0062

Shekhar, R., & Zagrodsky, V. (2002). Mutual information-based rigid and nonrigid registration of ultrasound volumes. *IEEE Trans. Med. Imag.* Vol.21, No.1, 9-22, ISSN: 0278-0062

Texas Instruments (1998). *TMS320C62x/67x Programmer's Guide, SPRU198D,* Texas Instruments Incorporated. Dallas, USA

Varela-Benítez, J. L., Gallegos-Funes, F. J., & Ponomaryov, V. I. (2007). Real-time speckle and impulsive noise suppression in 3-D imaging based on robust linear combinations of order statistics, *Proc. SPIE Real-Time Image Processing 2007*, Vol.6496, ISBN:9780819466099, pp. 64960H, San Jose, USA

Webb, A. G. (2002). *Introduction to Biomedical Imaging,* Wiley-IEEE Press, ISBN: 0471237663, *Hoboken, New Jersey*, USA
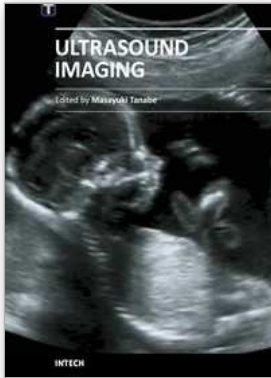
Ultrasound Imaging

Edited by Mr Masayuki Tanabe

In this book, we present a dozen state of the art developments for ultrasound imaging, for example, hardware implementation, transducer, beamforming, signal processing, measurement of elasticity and diagnosis. The editors would like to thank all the chapter authors, who focused on the publication of this book.

How to reference

In order to correctly reference this scholarly work, feel free to copy and paste the following:

Francisco J. Gallegos-Funes, Jose M. de-la-Rosa-Vazquez, Alberto J. Rosales-Silva and Suren Stolik Isakina (2011). Real-Time Speckle and Impulsive Noise Suppression in 3-D Ultrasound Imaging, Ultrasound Imaging, Mr Masayuki Tanabe (Ed.), ISBN: 978-953-307-239-5, InTech, Available from: http://www.intechopen.com/books/ultrasound-imaging/real-time-speckle-and-impulsive-noise-suppression-in-3-d-ultrasound-imaging

INTECH
open science | open minds